# THE TARGET DETECTION ON THE SEA SURFACE BASED ON THE MAXIMUM EIGENVALUE OF THE POLARIZATION COVARIANCE MATRIX

***Pham Trong Hung***
*Military Technical Academia, Ph-D-student, MA, Vietnam Republic*
***Nguyen Tien Tai***
*Ph-D, Military Technical Academia Vietnam Republic*
***Nguyen Trung Thanh***
*Ph-D, Military Technical Academia Vietnam Republic*

**ABSTRACT**

This paper proposes a novel method to detect small sea targets, using polarimetric radar. The maximum eigenvalue of the polarization covariance matrix is ultilized for the detection. In order to evaluate the new algorithm in practical applications, the real data collected from polarimetric IPIX radar at MC Master University has been tested with the new algorithm, and the result is displayed on the radar screen. The results of this method is also compared with those of the DoP and SP-GLR methods. Initial results show that the novel method significantly improves the detectability of small sea targets on the sea surface.

**1. Introduction**

Because of the strong fluctuation and the inhomogeneous property of the sea surface, the detection of small sea targets has always been a problem with sea radar systems, even with the detection based on the Doppler effect. In this situation, polarimetric information could be a useful and important tool to improve the detectability.

Since the optimum detector was proposed by Novak 1989 [1], several polarimetric algorithms have been developed [2], [3], [4]. Most of them ultilizes general likelihood ratio test [5], under the assumption that covariance matrix of the background clutter can be calculated by the training data, and this is considered as prior knowledge. Detection performance of those detectors decrease significantly in inhomogeneous and non-stationary clutter environment [6].

In order to address this problem, paper [1] proposes the use of the complex Gaussian distribution to model the inhomogeneous property of the background clutter. However, the use of this non- Gaussian distribution model increases the complexity of the optimum detection algorithm. For example, the detection statistic based on the proposal scheme in [7] works only for a special case of two polarimetric channels, and the detector in [8] does not support CFAR property.

Another approach to solve this problem is to use the degree of polarization (DoP) for the detection, as suggested in [9]. With this approach, however, the probability of detection is low and the false alarm rate is reasonably high. The authors of [10] proposed the use of the Weighted Average $H$ **(**$WAH$**)** and the Weighted Average $\bar{\alpha}$ **(**$WA\bar{\alpha}$**)**. The test results with real data shows this method has a high false alarm rate.

The maximum eigenvalue of the 2x2 covariance matrix of the multiple channels SAR is the informative parameter which has been widely used in the SAR applications such as Ground Moving Target Indication (GMTI) [11], polarimetric SAR [12], interferometry SAR [13], POLinSAR [14], change detection [15].

In this paper, the authors propose the detector based on the maximum eigenvalue of the polarimetric covariance matrix, in which the decision-making capability depends only on the data collected from the cell under test (CUT) but not on the secondary data or the prior knowledge of the target and background clutter. With this property, the systems is not vulnerable to inhomogeneous and non-stationary clutter.

The remainder of this paper is organized as follows: section II reviews of the methodology needed to obtain the maximum eigenvalue of the polarization covariance matrix. Sections III proposes a test procedure to detect target on the sea surface based on the maximum eigenvalue. Experimental results of the target detection on sea surface of this method with real data is presented in section IV, and the conclusion is provided in Section V.

**2. The maximum eigenvalue of the polarization covariance matrix**

***a. Eigenvalues and eigenvectors of polarization covariance matrix***

All the elements of the *m*-dimensional multi-channel system can be **transformed** into *m*-dimensional vector. If each element follows the complex Gaussian distribution with the zero mean, the vector *k* is said to follow a *m*-dimensional multivariate Gaussian distribution with zero mean and the covariance matrix $\Sigma$ and it can be represented as $k \sim N_m^C(0, \Sigma)$ [16].

For the Gaussian distribution with zero mean, the covariance matrix fully **describes the** data, playing an important role in many application fields. However, in practical situations, the real covariance matrix $\Sigma$ is unknown and must be estimated by its **maximum likelihood estimator** (MLE), the sample covariance matrix $Z = (1/n)\sum_{j=1}^{n} k_j k_j^{\dagger}$, where *n* is the number of estimated samples and † is the transpose conjugate operator.

The elements of Z follow the complex *m*-dimensional Wishart distribution with ***n* degree of freedom,** and the real covariance matrix $\Sigma$ is described by $Z \sim W_m^C(n, \Sigma)$ and defined as:

$$p_z(\mathrm{Z}) = \frac{n^{mn}\left|Z\right|^{n-m} etr(-\mathrm{n}\Sigma^{-1}\mathrm{Z})}{\left|\Sigma\right|^{n}\tilde{\Gamma}_m(n)} \text{ where}$$

$$\tilde{\Gamma}_m(n) = \pi^{m(m-1)/2}\prod_{i=1}^{m}\Gamma(n-i+1) \quad (1)$$

and Γ(.) is the Gamma function and *etr*(.) is exponential trace of a matrix.

From spectral theorem in linear algebra, we can decompose a full rank of *m*-dimensional covariance matrix in a set of *m* one-rank covariance matrices using its eigenvalues and eigenvectors. So that the real covariance matrix $\Sigma = \sum_{i=1}^{m} l_i(\mathrm{e}_i\mathrm{e}_i^{\dagger})$ and its estimators $Z = \sum_{i=1}^{m}\lambda_i(\mathrm{e}'_i\mathrm{e}'^{\dagger}_i)$ are given by:

$$\Sigma = Q\begin{bmatrix} l_1 .... & 0 \\ 0 & .... \\ 0 & .... \end{bmatrix} Q^{\dagger} \text{ và } Z = Q'\begin{bmatrix} \lambda_1 .... & 0 \\ 0 & .... \\ 0 & .... \end{bmatrix} Q'^{\dagger}, \quad \begin{matrix} Q = [e_1, e_2, ..., e_m] \\ Q' = [e_1', e_2', ..., e_m'] \end{matrix} \quad (2)$$

with their real non-negative eigenvalues $l_i$ and $\lambda_i$, and respective eigenvectors $e_i$ and $e_i'$.

***b. Statistical characteristics of the maximum eigenvalue of the covariance matrix***

Assume $k \sim N_m^C(0,\Sigma)$ is the *m*-dimensional complex vector whose elements follow the complex Gaussian distribution with the zero mean and the $m \times m$ dimensional covariance matrix $\Sigma$. Let $\Sigma$ has $l_m \le \cdots \le l_1$ eigenvalues, then the Cumulative Density Function (CDF) of the maximum eigenvalue of the sample covariance matrix $\langle kk^{\dagger}\rangle_n$ with $m \le n$ is given by:

$$F_{\lambda_{\max}}(x) = S\left|\Psi(x)\right|; \text{ with } S = \frac{\pi^{m(m-1)}n^{m(2\mathrm{n}-\mathrm{m}+1)/2}}{\tilde{\Gamma}_m(m)\tilde{\Gamma}_m(\mathrm{n})}\frac{\prod_{k=1}^{m-1}k^{m-k}}{\prod_{i=1}^{m}l_i^n\prod_{i<j}^{m}\left(\frac{1}{l_j}-\frac{1}{l_i}\right)}$$

where $\Psi(x)$ is the a $m \times m$ matrix with its $(i,j)$th element is $\Psi(x)_{i,j} = \frac{\gamma(n+1-j, x\frac{n}{l_i})}{\left(\frac{n}{l_i}\right)^{(n+1-j)}}$, and $\gamma$ is the incomplete Gamma function [17].

The probability density function (PDF) of the $\lambda_{max}$ of the sample covariance matrix $\langle kk^{\dagger}\rangle_n$ is:

$p_{\lambda_{\max}}(x) = S\left|\Psi(x)\right| tr\left[\Psi(x)^{-1}\Omega(x)\right]$ where $\Omega(x)$ is a $m \times m$ matrix with its $(i,j)$th elements $\Omega(x)_{i,j} = \exp\left(-\frac{n}{l_i}x\right)x^{n-j}$.

***c. The eigenvalues of the polarization covariance matrix***

The scattering matrix $S = \begin{bmatrix} s_{hh} & s_{hv} \\ s_{vh} & s_{vv} \end{bmatrix}$ is normally used to describe the relation between transmitting and back scattering fields. With common monostatic radar we have $s_{hh}$=$s_{vh}$. The received signals were range-processed and integrated to form an estimate for the 3-dimensional Pauli scattering vectors [18] at each range bin:

$$k_i = \frac{1}{\sqrt{2}}\left[(\mathrm{s}_{hh}+\mathrm{s}_{vv})\ (\mathrm{s}_{hh}-\mathrm{s}_{vv})\ 2\mathrm{s}_{hv}\right]^T \quad (3)$$

The $3 \times 3$ dimensional polarimetric coherency matrices can be calculated as:

$$\left\langle\left|T_3\right|\right\rangle = \frac{1}{N}\sum_{i=1}^{N}k_ik_i^H$$

$$= \frac{1}{2}\begin{bmatrix} \left\langle\left|s_{hh}+s_{vv}\right|^2\right\rangle & \left\langle(\mathrm{s}_{hh}+\mathrm{s}_{vv})(\mathrm{s}_{hh}-\mathrm{s}_{vv})^*\right\rangle & \left\langle 2(\mathrm{s}_{hh}+\mathrm{s}_{vv})s_{hv}^*\right\rangle \\ \left\langle(\mathrm{s}_{hh}-\mathrm{s}_{vv})(\mathrm{s}_{hh}+\mathrm{s}_{vv})^*\right\rangle & \left\langle\left|s_{hh}-\mathrm{s}_{vv}\right|^2\right\rangle & \left\langle 2(\mathrm{s}_{hh}+\mathrm{s}_{vv})s_{hv}^*\right\rangle \\ \left\langle 2s_{hv}(\mathrm{s}_{hh}+\mathrm{s}_{vv})^*\right\rangle & \left\langle 2s_{hv}(\mathrm{s}_{hh}-\mathrm{s}_{vv})^*\right\rangle & \left\langle 4\left|s_{hv}\right|^2\right\rangle \end{bmatrix} = \begin{bmatrix} T_{11} & T_{12} & T_{13} \\ T_{21} & T_{22} & T_{23} \\ T_{31} & T_{32} & T_{33} \end{bmatrix} \quad (4)$$

The eigenvalues of the $T_3$ matrix can be calculated from the equation:

$$T_3 - \lambda I = 0 \quad (5)$$

where $I$ is the unitary matrix and $\lambda$ is the eigenvalue of the $T_3$ matrix.

Equation (3) can be organized to the following equation:

$$a\lambda^3 + b\lambda^2 + c\lambda + d = 0 \quad (6)$$

where:

$a = 1$

$b = -(\mathrm{T}_{11} + \mathrm{T}_{22} + \mathrm{T}_{33})$

$c = (\mathrm{T}_{11}T_{22} + \mathrm{T}_{22}\mathrm{T}_{33} + \mathrm{T}_{33}\mathrm{T}_{11}) - (\mathrm{T}_{23}T_{32} + \mathrm{T}_{21}\mathrm{T}_{12} + \mathrm{T}_{12}\mathrm{T}_{31})$

$d = (\mathrm{T}_{11}T_{23}T_{32} + \mathrm{T}_{33}\mathrm{T}_{21}\mathrm{T}_{12} + \mathrm{T}_{22}\mathrm{T}_{12}\mathrm{T}_{31}) - (\mathrm{T}_{11}T_{22}T_{33} + \mathrm{T}_{12}\mathrm{T}_{23}\mathrm{T}_{31} + \mathrm{T}_{12}\mathrm{T}_{21}\mathrm{T}_{32})$

The eigenvalues can be extracted as the roots of equation (6):

$$\lambda_k = 2\sqrt{-\frac{p}{3}}\cos\left[\frac{1}{3}\mathrm{ar}\cos\left(\frac{3q}{2p}\sqrt{-\frac{p}{3}}\right) - \frac{2\pi k}{3}\right] - \frac{b}{3a} \text{ with } k = 0,1,2 \quad . (7)$$

where: $p = \dfrac{3ac - b^2}{3a^2}$; $q = \dfrac{2b^3 - 9abc + 27a^2d}{27a^3}$.

When $k = 0$, the maximum eigenvalue is:

$$\lambda_0 = 2\sqrt{-\frac{p}{3}}\cos\left[\frac{1}{3}\mathrm{ar}\cos\left(\frac{3q}{2p}\sqrt{-\frac{p}{3}}\right)\right] - \frac{b}{3a} \quad (8)$$

From the values of $\lambda_k$, the entropy *H* and $\alpha$ can be deduced. These parameters are also ultilized for the detection problems as in [18].

**3. The detection test**

In this section, the authors develop the detection test. The question here is to determine if a target is present within CUT or not, based on the data received. In other words, the detection **problem consists of choosing between two possible** hypotheses: hypothese $H_0$ (no target presense) and hypothese $H_1$ (target presense)

$$\begin{cases} H_0: & \lambda_{max} < \lambda_{ng} \\ H_1: & \lambda_{max} \geq \lambda_{ng} \end{cases} \quad (9)$$

The optimal detector ultilises the likehood ratio test [1], in that the optimal detector produces the maximum probability of detection ($P_D$) with the given false alarm rate ($P_{FA}$). In this case, however, there is no prior knowledge about the data distribution. As a result, the likehood ratio test cannot be applied in our problem Another method is the **general likehood ratio test (GLRT),** in which the unknown parameters of the data distribution are replaced by their **maximum likelihood estimated (MLE)** values in the likelihood ratio test [20].

**4. The performance of the test with the experimental data**

In this section, the authors use the training data taken from IPIX radar at McMaster University, Canada. The radar is located at the shore of the Atlantic Ocean, 30 m above the sea level. This is a **coherent and dual linear polarization** radar, allowing receive a **fully** polarimetric matrix within two transmitted pulses.

In this paper, data from files No54, No40 and No320 are analysed, each file contains data from 14 consecutive range cells. The small target is a spherical block of Styrofoam, wrapped with wire mesh and has one metre diameter. The target is located only in 8th cell, corresponding to the range of 2680m.

Each range cell contains 131072 samples (equivalent to 131 seconds) and 4 polarimetric channels: HH, HV, VH, VV. The parameters are shown in Table 1. The target can also be seen in cell number 7, 9 or 10. The data is collected in the condition that the sea wave is 0.7 m high.

The average target to clutter ratio varies in the range of 0-6 dB. The radar range resolution is 30 m and is sampled at every 15m. Radar works at frequency of 9.39 GHz, and the PRF of 1000 Hz. The training data is tested with the new method and the result is then compared with results of the DoP method [9]. The detection thresholds are set accordingly so that the false alarm rates in all three cases are $P_{FA} \approx 0.07$. Results are illustrated in Figure 1.

*Table 1* [21].

| Name | Data set No54 | Data set No40 | Data set No320 |
|---|---|---|---|
| Day | 1193.11.11 | 1993.11.10 | 1993.11.18 |
| Time | 16:36 | 00:16 | 17:42 |
| Target location | 2660 m, 128° | 2660 m, 128° | 2655 m, 170° |
| Range resolution | 30 m | 30 m | 30 m |
| Wave height (m) | 0.7 | 0.9 | 0.91 |
| Wind speed | 5.6 km/h | 2.5 km/h | 7.5 km/h |
| Sea state | 2 | 2 | 2 |

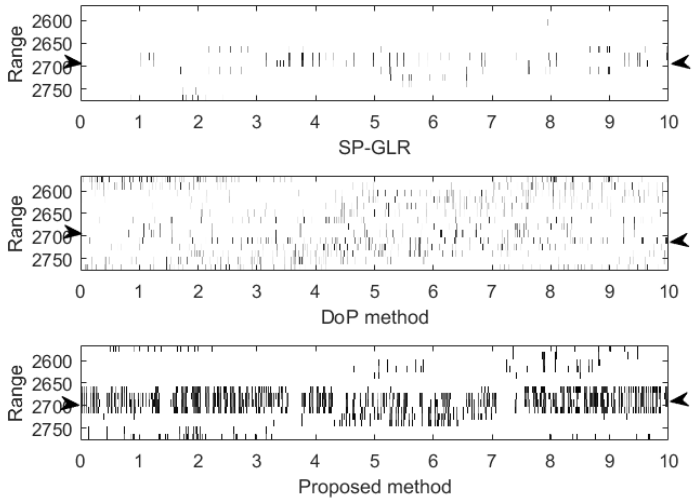


*Fig 1. Radar images in the range-time plot with experimenta data from IPIX radar, No54. The dark pixels correspond to the statistics higher than the thresold. The target location with the mark '>' and '<'.*

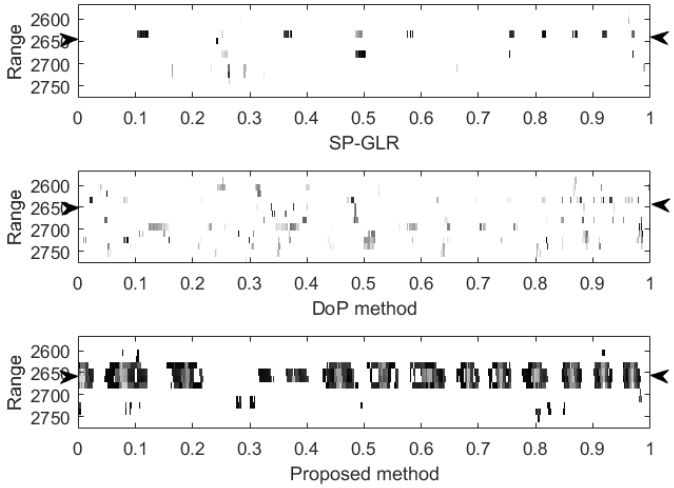


*Fig 2. Radar images in the range-time plot with experimenta data from IPIX radar, No40. The dark pixels correspond to the statistics higher than the thresold. The target location with the mark '>' and '<'.*

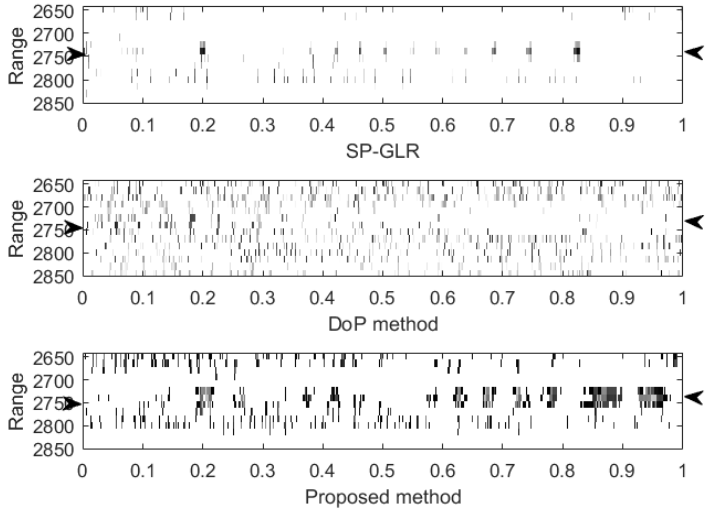


*Fig 3. Radar images in the range-time plot with experimenta data from IPIX radar, No320. The dark pixels correspond to the statistics higher than the thresold. The target location with the mark '>' and '<'.*

The Fig 1 shows the detection results on the sea surface with the proposed method and the others previously published polarimetric detectors in inhomogeneous environment. The dark pixels correspond with range cells which have statistics greater than the threshold. In the Fig 1, with the data file No54, Nov.11, also shows that the proposed method can detect the target with more visible than the others and the number of false alarm pixels is less than the others methods.

On the other hand, the DoP method has higher false alarm rate because of the inhomogeneous property of the sea surface. The SP-GLR method has the lower false alarm rate than that of the DoP method, however still higher than that of proposed method. Figure 2 corresponds to the data file No40, in which the wave height is higher and the wind speed is lower compared to data file No40 as shown in Table 1. The all three methods are tested in such condition and results are compared. The false alarm rate of the DoP and the SP-GLR methods are decreased, but the probabilities of the detection are also be reduced. The false alarm rate of the proposed method, on the other hand, has decreased as the DoP and SP-GLR but the probability of detection still remains high and the mark of the target is clearly visible as that of the data file N054.

In the end, the all three methods are tested with the data package No320, in which both the wave hight and the wind speed are higher than those of the two previous cases. Resuts show that the performances of all three methods decrease. The SP-GLR and DoP methods can hardly detect the target while the proposed method can detect the the target but with higher false alarm rate.

Another approach to evaluate the performance of the three methods is using the real data to plot the $P_D$ versus $P_{FA}$. This graphic is called Receiver Operating Characteristic (ROC) that means to describe the dependence of $P_D$ on $P_{FA.}$ The ROC here can be considered as empirical ROC because the values of $P_D$ and $P_{FA}$ are received from real data. Figure 4 shows the relation between $P_D$ and $P_{FA}$ for all three detectors.

Because the location of the target on the data is known, we can divide the graph into two areas: target and background clutter. The $P_D$ of the data on the area which contains the target is calculated by counting number of pixels has statistical values greater than the threshold. Similarly, the $P_{FA}$ can be calculated from data of the background clutter area. Each pair of ($P_D$, $P_{FA}$) corresponds to one point in the ROC graph. By changing the threshold, any point of the ($P_D$, $P_{FA}$) pairs are changed accordingly.

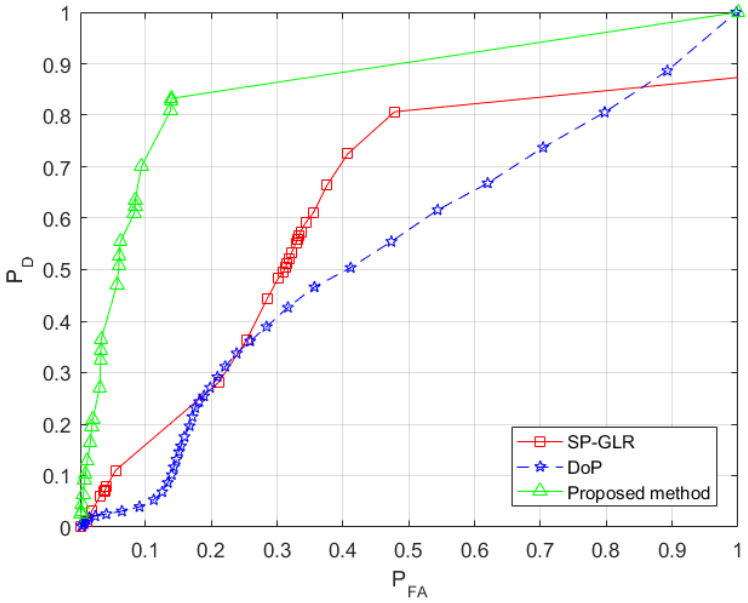


*Fig 4. Empirical receiver operating characteristic curves for the IPIX radar dataset No54*

Figure 4 shows that if $P_{FA}$<0.2, the $P_D$ of the SP-GLR method is quite low at 0.3, the same as of the DoP method. The proposed method, on the other hand, has significantly higher $P_D$ than other 2 methods. More specifically, with $P_{FA}$=0.2 and 0.1, the proposed method has $P_D$=0.85 and 0.7, respectively. Those values can be accepted on detecting the small RCS targets in such condition described as above.

**5. Conclusion**

The paper proposed a new method to detect target on the sea surface based on the maximum eigenvalue of the polarimetric covariance matrix. The real data is applied to the proposed method and the results is compared with the DoP and SP-GLR methods. The performance of the proposed method, the DoP and SP-GLR methods are also evaluated and compared by the empirical ROC graph. Results showed that the porposed method improved significantly the detectability of the small target on the sea surface.

**References**

[1] Novak L. M. en Sechtin M. B., „Studies of target detection algorithms that use polarimetric radar data," IEEE Trans. on Aerosp. Electron. Syst, vol. 25, nr. 2, Mar. 1989., pp. 150-165, 1989.

[2] Park H. R, Li J en Wang H, „Polarization-space-time domain generalized likelihood ratio

detection of radar targets," Signal Processing, vol. 41, p. 153—164, 1995.

[3] Pastina D, Lombardo P en Bucciarelli T, „Adaptive polarimetric target detection with coherent radar. Part I: Detection against Gaussian background," IEEE Trans. on Aerosp. Electron. Syst, Vols. %1 van %237, No. 4, pp. 1194-1206, 2001.

[4] Hurtado. M en Nehoira. A, „Polarimetric detection of target in heavy inhomogenous clutter," IEEE Transactions on Signal Processing, vol. 56, nr. 4, pp. 1349-1361, 2008.

[5] Kelly E. J, „An adaptive detection algorithm," IEEE Transactions on Aerospace and Electronic Systems, AES-22, vol. 1, p. 115—127, 1986.

[6] Park. H en Wang. H, „Adaptive polarization-space-time domain radar target detection in inhomogeneous clutter enviroments," Inst. Elect. Eng. Proc. Radar Sonar Navig., vol. 153, pp. 35-43, 2006.

[7] Lombardo. P, Pastina. D en Bucciarelli. T, „Adaptive polarimetric target detection with coherent radar. Part II: Detection against non-Gaussian background," IEEE Trans. Aerosp. Electr. Syst, vol. 37, pp. 1207-1220, 2001.

[8] De Maio.A en Alfano. G, „Polarimetric adaptive detection in non-Gaussian noise," Signal Processing, vol. 83, pp. 297-306, 2003.

[9] Bo Ren, Longfei Shi en Guoyu Wang, „Polarimetric Target Detection Using Statistic of the Degree of Polarization," Progress In Electromagnetics Reserch M, vol. 46, pp. 143-152, 2016.

[10] Peng Wu, Jun Wang en Wenguang Wang, „A Novel Method of Small Target Detection in Sea Clutter," International Scholarly Research Network ISRN Signal Processing, vol. 33, nr. 4, pp. 816-822, 2011.

[11] Nadarajah S, „Comments on Eigendecomposition of multi-channel covariance matrix with applications to SAR-GMTI," Signal processing, vol. 87, pp. 1534-1536, 2007.

[12] Hajnsek, L, Pottier, E en Cloude, S.R, „Inversion of surface parameters from polarimetric SAR," IEEE Trans Geosci. Remote Sens, vol. 4, pp. 727-744, 2003.

[13] Li, Z, Bao, Z, Li, H en Liao, G, „Image autocoregistration and InSAR interferogram estimation using joint subspace projection," IEEE Trans. Geosci. Remote Sens, vol. 44, pp. 288-297, 2006.

[14] Erten, E, Reigber, A, Ferro-Famil, L en Hellwich, O, „A new coherent similarity measure for temporal multichannel scene characterization," IEEE Trans. Geosci. Remote Sens, vol. 50, pp. 1-13, 2011.

[15] Zandona-Schneider, R en Fernandes, D, „Entropy Concept for Change Detection in Multitemporal SAR Images," in In Proceeding of EUSAR, Koln, Germany, 2002.

[16] R. Muirhead, Aspects of Multivariate Statistic Theory, New York, NY, USA: John Wiley&Sons, 1982.

[17] L. Andrews, Special Functions of Mathematics for Engineers, New York, NY, USA: McGraw-Hill Publishing Co, 1992.

[18] Cloude S.R en Pottier E, „An entropy based classification scheme for land applications of polarimetric SAR," IEEE Transactions on Geoscience and Remote Sensing, vol. 35, nr. 1, pp. 68-78, 2008.

[19] S. Kay, Fundamentals of Statistical Signal Processing: Detection Theory, NJ: Prentice-Hall: Englewood Cliffs, 1993.

[20] Kay S.M, Fundamentals of Statistical Signal Processing: Estimation Theory, Englewood Cliffs, NJ: Prentice-Hall, 1993.

[21] Haykin. S, „Information on: http://soma.ece.mcmaster.ca/ipix/dartmouth/datasets.html".

# ИССЛЕДОВАНИЯ И РАЗРАБОТКА С ИСПОЛЬЗОВАНИЯ ИННОВАЦИОННЫХ ТЕХНОЛОГИИ ПРОИЗВОДСТВА БЛЮД РУССКОЙ КУХНИ В ИНДУСТРИИ РЕСТОРАННОГО БИЗНЕСА

***Баянов Константин Олегович***

**Аннотация:** В последнее время наблюдается большой скачок технологий в приготовлении блюд, а также меняется понимание кулинарии в глазах гостей ресторанов. Не смотря на такой прогресс, развитие гастрономии в России, а в частности в регионах страны, находится не в лучшем состоянии. Данная ситуация складывается по ряду причин: нехватка высокопрофессионального персонала, приоритет получения прибыли, качество обслуживания. Особенно требуется уделять внимание национальной русской кухне.

**Ключевые слова:** кухня, репа, свекла, инновации, питание, агар-агар

Традиционная кухня это совокупность традиций и рецептов приготовления пищи, обусловленных историческими, географическими и иными условиями. Такие кухни имеют этнические, региональные и иные особенности. Но на сегодняшний день человечеству «приелось» традиционная кухня, поэтому, сначала, возникло направление в этой индустрии как высокая кухня - кухня «больших» заведений, изысканных ресторанов и роскошных отелей по всему миру. Она характеризуется тщательным приготовлением и тщательной презентацией продуктов питания, как правило, очень дорогих, и в сопровождении редких вин. Но и это не стало вершиной. Помимо внешнего вида блюда, люди стали изменять ее химический состав, что привило к возникновению молекулярной кухни. В связи с этим возник вопрос, в каком направлении стоит создавать заведение общественное питание,